Reliability-Based Analysis and Design of Strip Footings against Bearing Capacity Failure

Dalia S. Youssef Abdel Massih[1]; Abdul-Hamid Soubra, M.ASCE[2]; and Bak Kong Low, F.ASCE[3]

Abstract: This paper presents a reliability-based approach for the analysis and design of a shallow strip footing subjected to a vertical load with or without pseudostatic seismic loading. Only the punching failure mode of the ultimate limit state is studied. The deterministic models are based on the upper-bound method of the limit analysis theory. The random variables used are the soil shear strength parameters and the horizontal seismic coefficient. The Hasofer-Lind reliability index and the failure probability are determined. A sensitivity analysis is also performed. The influence of the applied footing load on the reliability index and the corresponding design point is presented and discussed. It was shown that the negative correlation between the soil shear strength parameters highly increases the reliability of the foundation and that the failure probability is highly influenced by the coefficient of variation of the angle of internal friction of the soil and the horizontal seismic coefficient. For design, an iterative procedure is performed to determine the breadth of the footing for a target failure probability.

DOI: 10.1061/(ASCE)1090-0241(2008)134:7(917)

CE Database subject headings: Bearing capacity; Earthquake loads; Limit analysis; Probability; Reliability; Shallow foundations; Punching; Failure loads.

Introduction

In the analysis and design of geotechnical structures, all the input data have some degree of uncertainty and, thus, may be considered as random variables or stochastic processes. Geotechnical engineers have always recognized the presence of uncertainty in their analysis and design. However, traditional deterministic models simplify the problem by considering the uncertain parameters to be deterministic and by accounting for the uncertainties through the use of a global safety factor, which is essentially a "factor of ignorance." This factor is derived based on past experience and does not reflect the inherent uncertainty of each parameter. A reliability-based analysis or design is more rational, since it takes into account the inherent uncertainty of each input variable. Nowadays, this is possible because of the improvement of our knowledge on the statistical properties of the soil (Phoon and Kulhawy 1999).

In the last decade, the reliability-based analysis has been extensively applied to the slope stability problem [see, for instance, Christian et al. (1994); Low and Tang (1997b,c); Low et al. (1998); Hassan and Wolff (1999); El-Ramly et al. (2002), (2003); among others]. However, very few authors have investigated the reliability-based analysis and design of foundations. Some (Griffiths and Fenton 2001; Fenton and Griffiths 2002, 2003, 2005; Griffiths et al. 2002; Przewlocki 2005; Popescu et al. 2005) modeled the uncertain parameters as random processes and examined the effect of the spatial variability of these parameters on the settlement or on the bearing capacity of foundations. Most of these studies considered the uncertainty of one single parameter (such as the soil elastic modulus, the cohesion, or the angle of internal friction of the soil). Others modeled the uncertainties of the different parameters as random variables and conducted reliability-based analysis using formulas of the bearing capacity factors (Cherubini 2000; Low and Phoon 2002). These approaches have the merit of simplicity, but also some shortcomings because they are based on approximate theoretical formulations.

In this study, a reliability-based analysis and design of a strip foundation resting on a $c-\varphi$ soil is presented. Two performance functions may characterize the footing behavior: The serviceability limit state and the ultimate limit state. Only the punching failure mode of the ultimate limit state is analyzed herein. Two loading cases are considered. The first examines the case of a strip footing subjected to a vertical load only; the second considers the case of a vertically loaded strip footing situated in a seismic area and subjected to a pseudostatic seismic loading. Two rigorous deterministic limit analysis models are used. The uncertainties of the soil shear strength parameters and the seismic coefficient are modeled as random variables. The basic concepts of the theory of reliability are described next, followed by the two deterministic models, and discussions of the probabilistic numerical results based on these models.

[1]Ph.D. Student, Univ. of Nantes and Lebanese Univ., BP 11-5147, Beirut, Lebanon. E-mail: Dalia.Youssef@univ-nantes.fr

[2]Professor, Institut de Recherche en Génie Civil et Mécanique, Univ. of Nantes, UMR CNRS 6183, Bd. de l'université, BP 152, 44603 Saint-Nazaire, France (corresponding author). E-mail: Abed.Soubra@univ-nantes.fr

[3]Associate Professor, School of Civil and Environmental Engineering, Nanyang Technological Univ., Nanyang Ave., Singapore 639798. E-mail: bklow@alum.mit.edu

Note. Discussion open until December 1, 2008. Separate discussions must be submitted for individual papers. To extend the closing date by one month, a written request must be filed with the ASCE Managing Editor. The manuscript for this paper was submitted for review and possible publication on March 21, 2006; approved on August 7, 2007. This paper is part of the ***Journal of Geotechnical and Geoenvironmental Engineering***, Vol. 134, No. 7, July 1, 2008. ©ASCE, ISSN 1090-0241/2008/7-917–928/$25.00.

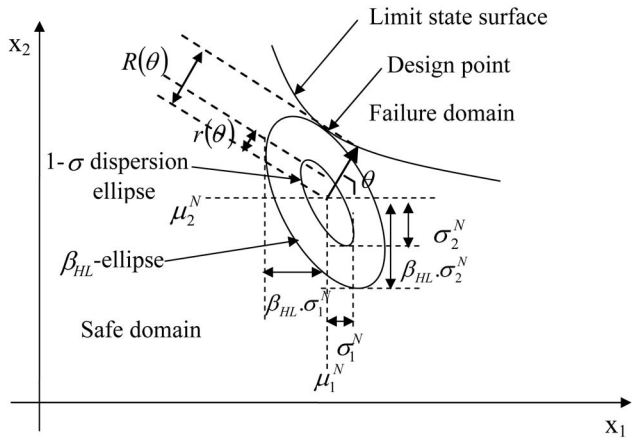

Fig. 1. Design point and equivalent normal dispersion ellipses in the space of two random variables

Basic Reliability Concepts

Two different measures are commonly used in the literature to describe the reliability of a structure: The *reliability index* and the *failure probability*.

Reliability Index

The reliability index of a geotechnical structure is a measure of the safety that takes into account the inherent uncertainties of the input variables. A widely used reliability index is the Hasofer and Lind (1974) index defined as the shortest distance from the mean value point of the random variables to the limit state surface in units of directional standard deviations, namely $\beta_{HL}=\min[R(\theta)/r(\theta)]$ (Fig. 1). Its matrix formulation is (Ditlevsen 1981)

$$\beta_{HL}=\min_{x\in F}\sqrt{(x-\mu)^T C^{-1}(x-\mu)} \tag{1}$$

in which x=vector representing the n random variables; μ=vector of their mean values; C=covariance matrix; and F=failure region. The minimization of Eq. (1) is performed subject to the constraint $G(x)\leqslant 0$ where the limit state surface $G(x)=0$, separates the n dimensional domain of random variables into two regions: A failure region F represented by $G(x)\leqslant 0$ and a safe region given by $G(x)>0$.

The classical approach for computing β_{HL} by Eq. (1) is based on the transformation of the limit state surface into the rotated space of standard normal uncorrelated variates. The shortest distance from the transformed failure surface to the origin of the reduced variates is the reliability index β_{HL}.

An intuitive interpretation of the reliability index was suggested in Low and Tang (1997a, 2004), where the concept of an expanding ellipse (Fig. 1) led to a simple method of computing the Hasofer-Lind reliability index in the original space of the random variables using an optimization tool available in most spreadsheet software packages. When there are only two uncorrelated nonnormal random variables x_1 and x_2, these variables span a two-dimensional random space, with an equivalent one-sigma dispersion ellipse [corresponding to $\beta_{HL}=1$ in Eq. (1) without the min.], centered at the mean values (μ_1^N, μ_2^N) and whose axes are parallel to the coordinate axes of the original space. For correlated variables, a tilted ellipse is obtained. Low and Tang (1997a, 2004) reported that the Hasofer-Lind reliability index β_{HL} may be regarded as the codirectional axis ratio of the smallest ellipse (which is either an expansion or a contraction of the $1-\sigma$ ellipse) that just touches the limit state surface to the $1-\sigma$ dispersion ellipse. They also stated that finding the smallest ellipsoid that is tangent to the limit state surface is equivalent to finding the most probable failure point.

Failure Probability

Given a vector of n random variables X and a performance function defined by $G(x)$, the failure probability P_f is defined by

$$P_f=\int_{G(x)\leqslant 0} f(x)dx \tag{2}$$

where $f(x)$=joint probability density function of the random variables X. By introducing the indicator function $I(x)$ defined as

$$I(x)=\begin{cases}1 & \text{if } G(x)\leqslant 0\\ 0 & \text{elsewhere}\end{cases} \tag{3}$$

The integral that gives the failure probability [Eq. (2)] can be written as

$$P_f=\int_{\Omega} I(x)f(x)dx \tag{4}$$

where Ω=total domain. A brief description of the methods used in this paper for the evaluation of this integral (i.e., FORM, MC, and IS) follows.

First-Order Reliability Method

From the first-order reliability method (FORM) and the Hasofer-Lind reliability index β_{HL}, one can approximate the failure probability as follows:

$$P_f\approx\Phi(-\beta_{HL}) \tag{5}$$

where $\Phi(\cdot)$=cumulative distribution function of a standard normal variable. In this method, the limit state function is approximated by a hyperplane tangent to the limit state surface at the design point.

Crude Monte Carlo Simulation

Monte Carlo is the most robust simulation method in which samples are generated with respect to the probability density of each variable. For each sample, the response of the system is calculated. An unbiased estimator of the failure probability is given by

$$\tilde{P}_f=\frac{1}{N}\sum_{i=1}^{N} I(x_i) \tag{6}$$

where N=number of samples and $I(x)$ is as defined in Eq. (3). The coefficient of variation of the estimator is given by

$$\mathrm{COV}(\tilde{P}_f)=\sqrt{\frac{(1-P_f)}{P_f N}} \tag{7}$$

Importance Sampling Simulation

Generally, for a given target of the coefficient of variation, the crude Monte Carlo simulation requires a large number of samples, i.e., a large computation time. This is especially the case for small values of the failure probability P_f. The importance sampling (IS) simulation method is a more efficient approach; it requires fewer

sample points than the crude Monte Carlo method. In this approach, the initial sampling density is shifted to the design point in order to concentrate the samples in the region of greatest probability density within the zone defined by $G(x) \leq 0$. The design point may be determined by using any of the classical methods such as Rackwitz-Fiessler algorithm (Rackwitz-Fiessler 1978), Low and Tang's ellipsoid approach (Low and Tang 1997a, 2004), etc. An estimator of the failure probability P_f is obtained as follows (Melchers 1999):

$$\tilde{P}_f = \frac{1}{N}\sum_{i=1}^{N} I(v_i)\frac{f(v_i)}{h(v_i)} \tag{8}$$

where $h(\cdot)$ = new sampling density centred at the design point, and v = vector of sample values with probability density function $h(\cdot)$. The coefficient of variation of the estimator is given by (Melchers 1999)

$$\mathrm{COV}(\tilde{P}_f) = \frac{1}{P_f}\sqrt{\frac{1}{N}\left[\frac{1}{N}\sum_{i=1}^{N}\left(I(v_i)\frac{f(v_i)}{h(v_i)}\right)^2 - (P_f)^2\right]} \tag{9}$$

Sensitivity Factors

The sensitivity factors convey the relative importance of the random variables in affecting reliability. The "omission sensitivity factor" is used in this paper. It gives the relative error in the reliability index when a random variable is replaced by its deterministic mean value. It is given by

$$\gamma_i(\mu_i) = \frac{\beta_{\mathrm{HL}}(x_i = \mu_i)}{\beta_{\mathrm{HL}}} \tag{10}$$

where β_{HL} = value of the reliability index calculated when all parameters are considered as random variables, and $\beta_{\mathrm{HL}}(x_i = \mu_i)$ = reliability index determined when x_i is replaced by its deterministic mean value.

Reliability Analysis of Shallow Strip Foundations

The aim of this paper is to perform a reliability analysis of a strip footing resting on a $c-\varphi$ soil and subjected to a vertical load. The case of a vertically loaded strip footing situated in a seismic area is also studied. Quasi-static representation of earthquake effects using the seismic coefficient concept is adopted. The earthquake acceleration for both the soil and the structure is assumed to be the same: Only the horizontal seismic coefficient K_h is considered, the vertical seismic coefficient often being disregarded. The deterministic models are based on the upper-bound method of the limit analysis theory (Soubra 1999). Due to uncertainties in soil shear strength parameters and horizontal seismic coefficient, the cohesion c, the angle of internal friction φ, and the seismic coefficient K_h are considered as random variables. The performance function used in the reliability analysis is defined with respect to the bearing failure of the soil. It is given as follows:

$$G = \frac{P_u}{P_S} - 1 \tag{11}$$

where P_u = ultimate foundation load, and P_S = applied load. One may use another performance function as $G = P_u - P_S$. However, this leads exactly to the same value of the reliability index since the Hasofer-Lind reliability index does not vary with alternative but equivalent definitions of the performance function. Notice, however, that the first definition has an advantage over the second one since it makes it possible to introduce the concept of the safety factor as follows: $G = F - 1$.

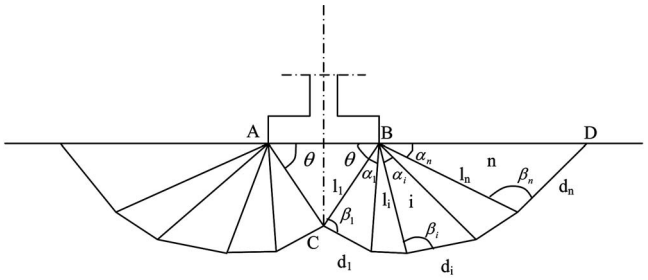

Fig. 2. Failure mechanism $M1$ for static bearing capacity analysis

Limit Analysis Models

Two deterministic models are used in this paper. In these models, the upper-bound theorem of limit analysis is applied to the bearing capacity problem of a strip footing using two kinematically admissible failure mechanisms referred to in the following as $M1$ and $M2$. These mechanisms were presented by Soubra (1999). The approach is simple and self-consistent and it obtains rigorous upper-bound solutions in the framework of limit analysis theory. Although the results given by this approach are upper-bound solutions, they are the smallest upper-bounds against the available ones given by rigid block mechanisms. In some cases (i.e., for weightless soil), they are the exact solutions, since they are equal to the results given by the lower-bound method.

$M1$ is a translational symmetrical multiblock failure mechanism (Fig. 2) and is used for the computation of the bearing capacity of a vertically loaded footing. $M2$ is a translational nonsymmetrical multiblock failure mechanism and is suitable for the calculation of the bearing capacity of vertically loaded foundations situated in seismic areas by a pseudostatic approach (Fig. 3). The calculation of the bearing capacity is performed by equating the total rate at which work is done by the foundation load, the soil weight in motion, the horizontal seismic loads (in the case of seismic loading), and the ground surface surcharge to the total rate of energy dissipation along the lines of velocity discontinuities. For both $M1$ and $M2$, it is found that an upper-bound on the bearing capacity of the soil is given as follows:

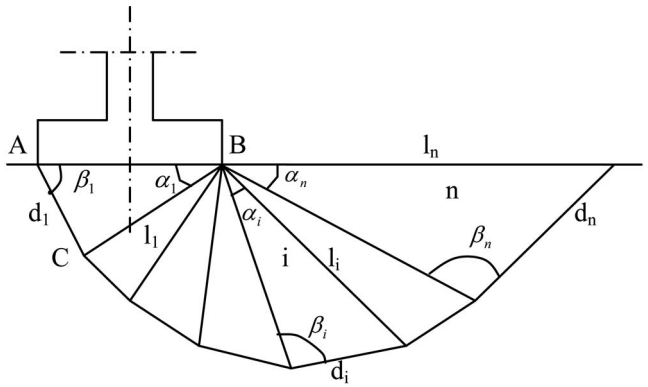

Fig. 3. Failure mechanism $M2$ for seismic bearing capacity analysis

$$P_u = \frac{1}{2}\gamma B^2 N_\gamma + qBN_q + cBN_c \tag{12}$$

in which the bearing capacity factors N_γ, N_q, and N_c can be expressed in terms of the geometrical parameters of each mechanism. For the $M1$ mechanism, these factors are given as follows:

$$N_\gamma = -(f_1 + f_2) \tag{13}$$

$$N_q = -f_3 \tag{14}$$

$$N_c = 2(f_4 + f_5 + f_6) \tag{15}$$

where the expressions of $f_i (i=1,\ldots,6)$ are given in Appendix I. For the $M2$ mechanism, the bearing capacity factors are given by

$$N_\gamma = -\frac{1}{\sin(\beta_1 - \varphi) + K_h \cos(\beta_1 - \varphi)}(g_1 + K_h g_2) \tag{16}$$

$$N_q = -\frac{1}{\sin(\beta_1 - \varphi) + K_h \cos(\beta_1 - \varphi)}(g_3 + K_h g_4) \tag{17}$$

$$N_c = \frac{1}{\sin(\beta_1 - \varphi) + K_h \cos(\beta_1 - \varphi)}(g_5 + g_6) \tag{18}$$

where the expressions of $g_i (i=1,\ldots,6)$ are given in Appendix II. The ultimate load of the foundation is obtained by minimization of Eq. (12) with regard to the mechanism's geometrical parameters. For further details on the failure mechanisms, the reader can refer to Soubra (1999).

Ellipsoid Approach via Spreadsheet

Low and Tang (1997a, 2004) showed that the minimization of the Hasofer-Lind reliability index can be efficiently carried out in the Excel spreadsheet environment. The spreadsheet approach is simple and easy to understand because it works in the original space of random variables and does not require the additional step of transforming x to u where u is a transformed vector of the random variables in the uncorrelated Gaussian space. However, the optimization in original space is not preferred from a computational perspective (STRUREL 1991). This is because optimization in standardized space is mathematically more desirable in nonlinear optimization. For example, when minimizing the quadratic form of Eq. (1) in the original space, in some cases the correct solution is obtained only when the solver option "use automatic scaling" is activated. As an alternative, Cholesky factorization of the convariance matrix can be used. The robustness of the latter approach is investigated in Phoon (2004).

When the random variables are nonnormal, the Rackwitz-Fiessler equivalent normal transformation was used to compute the equivalent normal mean μ_x^N and the equivalent normal standard deviation σ_x^N. The iterative computations of μ_x^N and σ_x^N for each trial design point are automatic during the constrained optimization search.

In the present paper, by the Low and Tang method, one literally sets up a tilted ellipsoid in the Excel spreadsheet and minimizes the dispersion ellipsoid subject to the constraint that it be tangent to the limit state surface using the Excel Solver with the automatic scaling option. Eq. (1) may be rewritten as (Low and Tang 1997c, 2004)

$$\beta_{HL} = \min_{x \in F} \sqrt{\left[\frac{x - \mu_x^N}{\sigma_x^N}\right]^T [R]^{-1} \left[\frac{x - \mu_x^N}{\sigma_x^N}\right]} \tag{19}$$

in which $[R]^{-1}$ = inverse of the correlation matrix. This equation will be used [instead of Eq. (1)] since the correlation matrix $[R]$ displays the correlation structure more explicitly than the covariance matrix $[C]$.

Additional information on Solver's options and algorithms can be found in the Microsoft Excel Solver's help file and at www.solver.com. The FORM implementation procedure in the spreadsheet is described in Low (2005) and Low and Tang (1997a,b,c, 2004). Some Excel files are available at http://alum.mit.edu/www/bklow.

Probabilistic Numerical Results

For both $M1$ and $M2$ failure mechanisms, the numerical results presented in this paper consider the case of a shallow strip foundation with breadth $B=2m$. The soil has a unit weight of 18 kN/m^3. No surcharge loading ($q=0$) is considered in the analysis. Different values of the coefficients of variation of the angle of internal friction and cohesion are presented in the literature. For most soils, the mean value of the effective angle of internal friction is typically between 20 and 40°. Within this range, the corresponding coefficient of variation as proposed by Phoon and Kulhawy (1999) is essentially between 5 and 15%. For the effective cohesion, the coefficient of variation varies between 10 and 70% (Cherubini 2000). For the coefficient of correlation, Harr (1987) has shown that a correlation exists between the effective cohesion c and the effective angle of internal friction φ. The results of Wolff (1985) ($\rho_{c,\varphi}=-0.47$), Yuceman et al. (1973) ($-0.49 \leq \rho_{c,\varphi} \leq -0.24$), Lumb (1970) ($-0.7 \leq \rho_{c,\varphi} \leq -0.37$), and Cherubini (2000) ($\rho_{c,\varphi}=-0.61$) are among the ones cited in the literature. In this paper, the illustrative values used for the statistical moments of the shear strength parameters and their coefficient of correlation $\rho_{c,\varphi}$ are as follows: $\mu_c=20$ kPa, $\mu_\varphi=30°$, $COV_c=20\%$, $COV_\varphi=10\%$, and $\rho_{c,\varphi}=-0.5$. These values are within the range of the values cited above.

Mechanism M1

For the configuration presented above, the ultimate footing load determined for the mean values of the soil shear strength parameters is $P_u=2{,}136.72$ kN/m. For the probability distribution of the random variables, two cases are studied. In the first case, referred to as *normal* variables, c and φ are considered as normal variables. In the second case, referred to as *nonnormal* variables, c is assumed to be lognormally distributed while φ is assumed to be bounded and a beta distribution is used (Fenton and Griffiths 2003). The parameters of the beta distribution are determined from the mean value and standard deviation of φ (Haldar and Mahadevan 2000). For both cases, correlated or uncorrelated variables are considered.

Probabilistic Failure Surface

The conventional deterministic approach for the calculation of a safety factor or an ultimate load on a soil mass is based on the minimization of these functions over a range of trial failure surfaces. The surface of minimum factor of safety or ultimate load is referred to as the critical deterministic surface. A common approach to determine the reliability of a stressed soil mass is based

on the calculation of the reliability index β_{HL} corresponding to this surface (Christian et al. 1994). In this paper, a more rigorous approach is used. It consists of the determination of the reliability index by minimizing the quadratic form of Eq. (19) not only with respect to the random variables, but also with respect to the geometrical parameters of the failure mechanism $(\theta, \alpha_i, \beta_i)$. Twelve rigid blocks (i.e., $n=12$ in Fig. 2) are considered for each side of the footing. Therefore, the minimization is performed with respect to 27 parameters $(\theta, \alpha_i, \beta_i, c, \varphi)$. The surface obtained corresponding to the minimum reliability index is referred to here as the critical probabilistic surface. The reliability index calculated with respect to the critical probabilistic surface is smaller (i.e., more critical) than the one calculated by using the critical deterministic surface. Had one considered the deterministic critical surface, a slightly higher reliability index value of 3.49 would have been obtained instead of 3.27 for the case with normal uncorrelated soil shear strength parameters. In all subsequent results, for both the $M1$ and $M2$ mechanisms, the reliability index is calculated using the probabilistic failure surface.

Reliability Index and Sensitivity Factors

Table 1 presents the Hasofer-Lind reliability index and the corresponding design point for different values of the vertical applied load P_S varying from small values up to the deterministic ultimate load. This ultimate load is the one for which the design point is equal to the mean point for normal variables and equivalent normal mean point for nonnormal variables. The table also gives the omission sensitivity factors of the angle of internal friction and the cohesion. All these results are presented for *normal* and *nonnormal*, correlated and uncorrelated shear strength parameters. For all cases, the reliability index decreases with the increase of the applied load P_S (i.e., with the decrease of the safety factor $F=P_u/P_S$) until it vanishes for an applied load equal to the deterministic ultimate load. This case corresponds to a deterministic state of failure for which $F=1$ using the mean values of the random variables and the failure probability is equal to 50%.

The comparison of the results of correlated variables with those of uncorrelated variables (Fig. 4) shows that the reliability indices corresponding to uncorrelated variables are smaller than those of negatively correlated variables for both *normal* and *nonnormal* variables. One can conclude that assuming uncorrelated shear strength parameters is conservative in comparison to assuming negatively correlated shear strength parameters. For instance, when the safety factor is equal to 4.27 (i.e., $P_S=500$ kN/m), the reliability index increases by 40% if the variables c and φ are considered to be negatively correlated. Fig. 4 also shows that for small values of the safety factor, the results of *normal* and *nonnormal* variables are nearly identical. A difference appears for large values of the safety factor.

From Table 1, when $P_S=700$ kN/m, the most probable failure point for uncorrelated and correlated *normal* variables is found to be at ($c^*=12.45$ kPa, $\varphi^*=22°$) and ($c^*=16.55$ kPa, $\varphi^*=19.88°$), respectively. These are the points of tangency of the $\beta_{HL}-\sigma$ ellipses with the limit state surface. Notice that the limit state surface divides the combinations of (c, φ) that would lead to failure from the combinations that would not. The (c, φ) values defining the limit state surface are obtained by searching c (or φ) for a prescribed φ (or c) that achieve both the conditions (i) a minimum ultimate load P_u and (ii) a safety factor $F=P_u/P_S=1$. For this purpose, a numerical procedure was coded in Microsoft Excel Visual Basic. It calls the Excel Solver iteratively in order to simultaneously satisfy the two conditions above. Fig. 5 provides graphical representation of the reliability analysis for both correlated and uncorrelated shear strength parameters in the physical space of the random variables. One can easily see that negative correlation between shear strength parameters rotates the major axis of the ellipse from the horizontal direction.

The values (c^* and φ^*) of the design points corresponding to different values of the vertical applied load can give an idea about the partial safety factors of each of the strength parameters c and $\tan\varphi$ as follows:

$$F_c = \frac{\mu_c}{c^*} \tag{20}$$

$$F_\varphi = \frac{\tan(\mu_\varphi)}{\tan\varphi^*} \tag{21}$$

For uncorrelated shear strength parameters, the values of c^* and φ^* at the design point are smaller than their respective mean values and increase with the increase of the applied load. For negatively correlated shear strength parameters, c^* slightly exceeds the mean for some values of the applied load.

The values of the omission sensitivity factors have shown that the effect of the randomness of the angle of internal friction on the reliability index is much more pronounced than that of the cohesion, especially for the case of *nonnormal* random variables.

Failure Probability

Figs. 6 and 7 present, respectively, the failure probability and the corresponding coefficient of variation as a function of the number of samples for both MC and IS simulations when the soil shear strength parameters are *normal* and uncorrelated and the footing applied load is equal to 700 kN/m. In this paper, MC and IS simulations were performed in the standardized space of uncorrelated variables. Hence, only uncorrelated normal random variables have been generated. For nonnormal and correlated variables, the limit state surface, which is determined point by point as explained in the previous section, is transformed to the standardized space of uncorrelated normal variables using the equivalent normal transformation (i.e., the Rackwitz-Fiessler equations) for each couple of (c, φ). The two equations used for the transformation of each (c, φ) of the limit state surface from the physical space to the standarized normal uncorrelated space (u_1, u_2) are (Lemaire 2005)

$$u_1 = \left(\frac{c-\mu_c^N}{\sigma_c^N}\right) \tag{22}$$

$$u_2 = \frac{1}{\sqrt{1-\rho^2}}\left[\left(\frac{\varphi-\mu_\varphi^N}{\sigma_\varphi^N}\right) - \rho\left(\frac{c-\mu_c^N}{\sigma_c^N}\right)\right] \tag{23}$$

where ρ=coefficient of correlation of c and φ; and μ_c^N, μ_φ^N, σ_c^N, and σ_φ^N=respectively, the equivalent normal means and standard deviations of the random variables c and φ. They are determined from the translation approach using the following equations:

$$\frac{c-\mu_c^N}{\sigma_c^N} = \Phi^{-1}[F_c(c)] \tag{24}$$

$$\frac{\varphi-\mu_\varphi^N}{\sigma_\varphi^N} = \Phi^{-1}[F_\varphi(\varphi)] \tag{25}$$

where F_c and F_φ=non-Gaussian cumulative distribution functions of c and φ; and $\Phi^{-1}(\cdot)$=inverse of the standard normal cumulative distribution. If desired, the original correlation matrix (ρ_{ij}) of the nonnormals can be modified to ρ'_{ij} in line with the equivalent

Table 1. Reliability Index and Sensitivity Factors

P_S (kN/m)	c^* (kPa)	φ^* (deg)	β_{HL}	$\gamma(\mu_c)$	$\gamma(\mu_\varphi)$	F_c	F_φ
(a) Uncorrelated normal variables							
500	8.87	20.69	4.17	1.30	1.39	2.25	1.53
700	12.45	22.00	3.27	1.21	1.60	1.61	1.43
900	14.76	23.47	2.54	1.16	1.81	1.35	1.33
1,100	16.35	24.84	1.95	1.13	2.01	1.22	1.25
1,300	17.49	26.08	1.45	1.11	2.20	1.14	1.18
1,500	18.35	27.19	1.02	1.09	2.38	1.09	1.12
1,700	19.00	28.17	0.66	1.08	2.56	1.05	1.08
1,900	19.52	29.06	0.34	1.08	2.74	1.02	1.04
2,100	19.93	29.86	0.05	1.02	2.91	1.00	1.01
2,136.72	20.00	30.00	0.00	—	—	1.00	1.00
(b) Correlated normal variables							
500	10.80	19.41	5.87	0.92	0.99	1.85	1.64
700	16.55	19.88	4.48	0.88	1.17	1.21	1.60
900	18.89	21.66	3.38	0.87	1.36	1.06	1.45
1,100	19.89	23.46	2.53	0.87	1.54	1.01	1.33
1,300	20.29	25.09	1.85	0.87	1.72	0.99	1.23
1,500	20.40	26.51	1.29	0.87	1.90	0.98	1.16
1,700	20.36	27.76	0.82	0.87	2.07	0.98	1.10
1,900	20.22	28.86	0.41	0.88	2.23	0.99	1.05
2,100	20.04	29.83	0.06	0.93	2.40	1.00	1.01
2,136.72	20.00	30.00	0.00	—	—	1.00	1.00
(c) Uncorrelated nonnormal variables							
500	12.46	18.35	4.59	1.20	5.44	1.61	1.74
700	14.39	20.98	3.41	1.18	5.27	1.39	1.51
900	15.76	23.02	2.58	1.15	4.87	1.27	1.36
1,100	16.80	24.67	1.94	1.13	3.89	1.19	1.26
1,300	17.60	26.04	1.42	1.12	3.51	1.14	1.18
1,500	18.25	27.22	0.99	1.12	3.29	1.10	1.12
1,700	18.77	28.25	0.62	1.13	3.16	1.07	1.07
1,900	19.21	29.15	0.30	1.19	3.03	1.04	1.04
2,100	19.59	29.96	0.02	1.37	2.17	1.02	1.00
2,114.15	19.61	30.00	0.00	—	—	1.02	1.00
(d) Correlated nonnormal variables							
500	14.99	16.77	6.20	0.89	4.03	1.33	1.92
700	17.41	19.45	4.51	0.89	3.99	1.15	1.63
900	18.82	21.68	3.34	0.89	3.76	1.06	1.45
1,100	19.57	23.59	2.47	0.89	3.05	1.02	1.32
1,300	19.92	25.22	1.79	0.89	2.80	1.00	1.23
1,500	20.01	26.64	1.23	0.90	2.66	1.00	1.15
1,700	19.96	27.88	0.77	0.92	2.57	1.00	1.09
1,900	19.82	28.97	0.37	0.97	2.49	1.01	1.04
2,100	19.63	29.95	0.02	1.13	1.80	1.02	1.00
2,114.15	19.61	30.00	0.00	—	—	1.02	1.00

normal transformation, as suggested in Der Kiureghian and Liu (1986). Some tables of the ratio ρ'_{ij}/ρ_{ij} are given in Appendix B2 of Melchers (1999), including closed form solution for the special case of lognormals. For the cases illustrated herein, the correlation matrix, thus modified, differs only slightly from the original correlation matrix. Hence, for simplicity, the examples in this study retain their original unmodified correlation matrices.

The importance sampling density function used is given in the standard uncorrelated space as follows (Lemaire 2005):

$$f(u) = \frac{1}{\sqrt{2\pi}} e^{-1/2(u-u^*)^2} \tag{26}$$

where u^*=transformed value of the design point in the standard uncorrelated space of the random variables. The convergence of the failure probability calculated by IS is achieved for a sample size of 20,000. The corresponding coefficient of variation is about 2%, which is smaller than the commonly adopted value used in

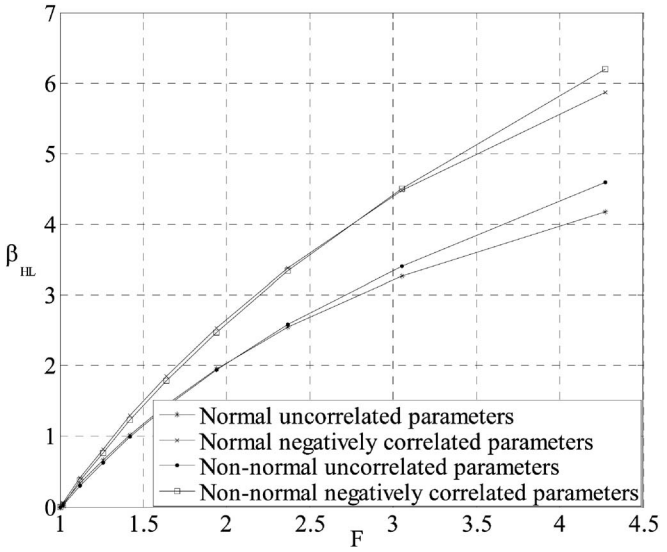

Fig. 4. Reliability index versus safety factor for $COV_c=20\%$, $COV_\varphi=10\%$

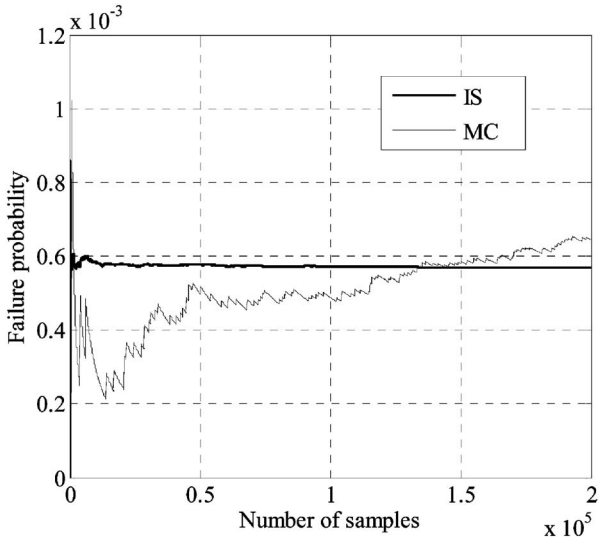

Fig. 6. Failure probability versus the number of samples

the literature (i.e., 10%). For the Monte Carlo simulation, a sample size of 5,000,000 is needed to achieve a constant value of the failure probability and a corresponding coefficient of variation of 2%. In order to have a clear visualization of the convergence of the IS method, the maximal number of samples represented on the *x*-axis of Figs. 6 and 7 was limited to 200,000. In the following, only IS simulation method will be used since it gives accurate results with reasonable sample size. All the subsequent calculations are performed for a coefficient of variation of the estimator of 2%.

By varying the target of the ultimate load, the reliability index is calculated and the CDF is plotted in Figs. 8 and 9 using FORM approximation and importance sampling (IS) simulation. From these figures, it is observed that the CDFs obtained from FORM approximation are in good agreement with those obtained from IS simulation for *normal, nonnormal*, uncorrelated, and correlated variables for the commonly used values of the coefficients of variation of the soil shear strength parameters (i.e., $COV_c=20\%$, $COV_\varphi=10\%$). This means that FORM approximation is an acceptable approach for estimating the failure probability for the commonly used values of the soil variability. In order to explain the good agreement between the two approaches, the limit state surface is plotted. Fig. 10 shows the limit state surface corresponding to an applied load $P_S=1{,}300$ kN/m for *nonnormal* correlated random variables in the standard space of normal uncorrelated variables. This figure also shows the linear FORM approximation, which is tangent to the limit state surface at the design point. From this figure, it can be shown that the linear FORM approximation is very close to the exact limit state surface within the circle centred at the origin of the rotated and transformed space and having a radius equal to 3. This explains why a good agreement between the two approaches is obtained. The difference between the two failure probabilities shown in Fig. 10 is 1.25%. For larger values of the coefficients of variation (i.e., $COV_c=50\%$, $COV_\varphi=20\%$), the difference between the two approaches increases and attains 3.32% as can be shown from the values given in Fig. 11. This can be explained by the curvature of the limit state surface near the design point. Since the limit state surface is convex with respect to the origin of the rotated and transformed space, the FORM approximation overestimates the failure probability.

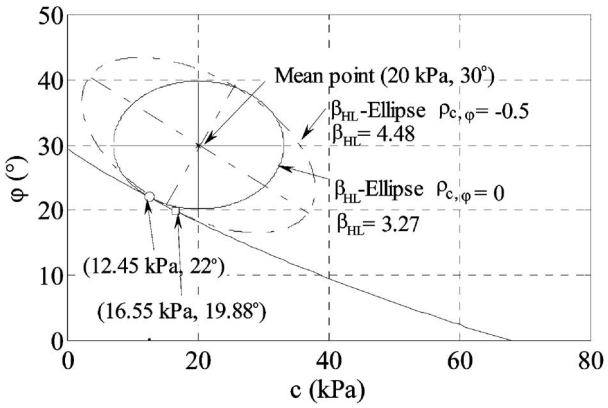

Fig. 5. β_{HL}—ellipses for correlated and uncorrelated variables in the physical space

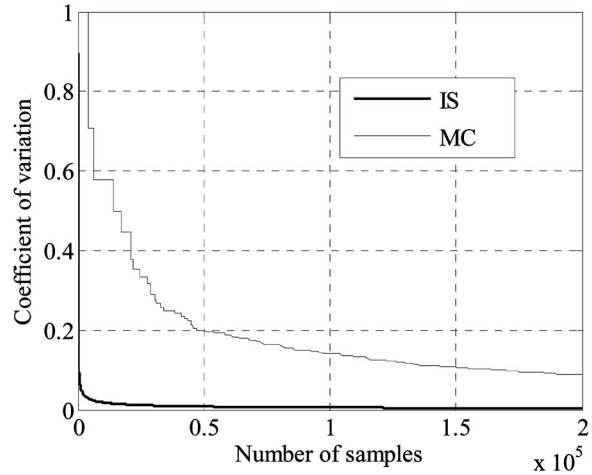

Fig. 7. Coefficient of variation of the failure probability versus the number of samples

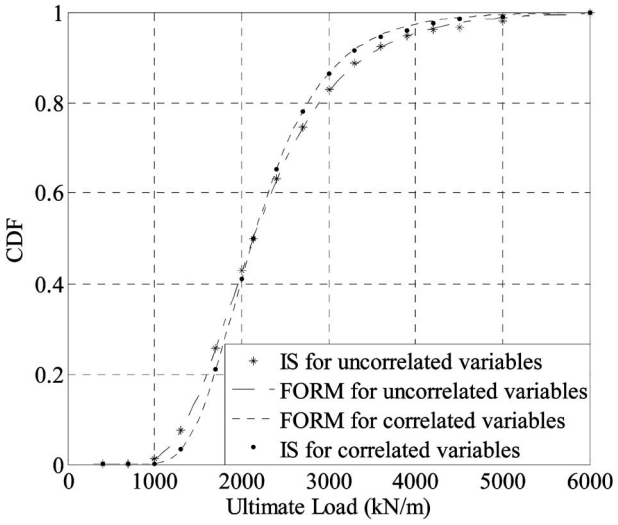

Fig. 8. Comparison of the CDFs of the ultimate load given by FORM and IS for *normal* variables

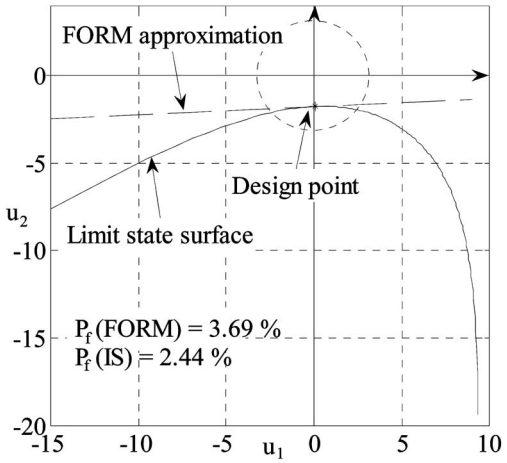

Fig. 10. Limit state surface and FORM approximation for *nonnormal* correlated variables, for $COV_c = 20\%$, $COV_\varphi = 10\%$

Fig. 12 presents the CDFs of the ultimate load for *normal, nonnormal*, correlated, and uncorrelated variables as given by FORM. When no correlation between shear strength parameters is considered, one can notice a more spread out CDF of the ultimate load (i.e., a higher coefficient of variation of the ultimate load). The chosen probability distribution (i.e., normal, lognormal, and beta distribution) does not significantly affect the values of the failure probability.

Fig. 13 presents the effect of the coefficient of variation of the shear strength parameters on the CDF of the ultimate load. It can be seen that a small change in the coefficient of variation of φ highly affects the CDF curve. On the other hand, the CDF curve is not sensitive to changes in the uncertainty of the cohesion. Thus, the failure probability is highly influenced by the coefficient of variation of φ. The greater the scatter in φ, the higher the failure probability. This means that accurate determination of the uncertainties of the angle of internal friction φ is very important in obtaining reliable probabilistic results. In contrast, the coefficient of variation of c does not significantly affect the failure probability.

Reliability-Based Design

The conventional approach used in the design of a shallow foundation is to prescribe a target safety factor (generally $F=3$) and to determine the corresponding breadth B of the footing. Recently, a reliability-based design approach (RBD) has been used by several authors [e.g., Low (2005) and Phoon et al. (2003), among others]. This approach was used in this section. It consists of the calculation of B for a target reliability index of 3.8 as suggested by Eurocode 7 for the ultimate limit states (Calgaro 1996). This foundation breadth is called hereafter "probabilistic foundation breadth."

Fig. 14 presents the probabilistic foundation breadth for different values of the coefficients of variation of the shear strength parameters and their coefficient of correlation. This figure also presents the deterministic breadth corresponding to a safety factor

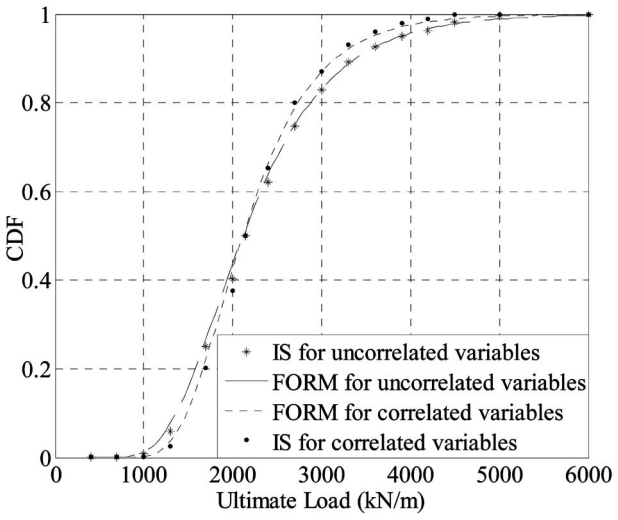

Fig. 9. Comparison of the CDFs of the ultimate load given by FORM and IS for *nonnormal* variables

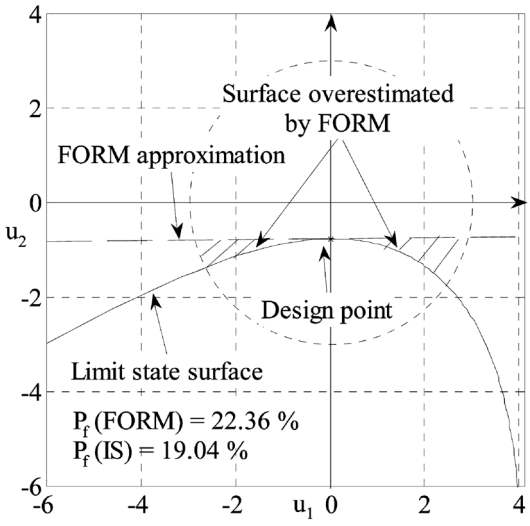

Fig. 11. Limit state surface and FORM approximation for *nonnormal* correlated variables and large coefficients of variation $COV_c = 50\%$, $COV_\varphi = 20\%$

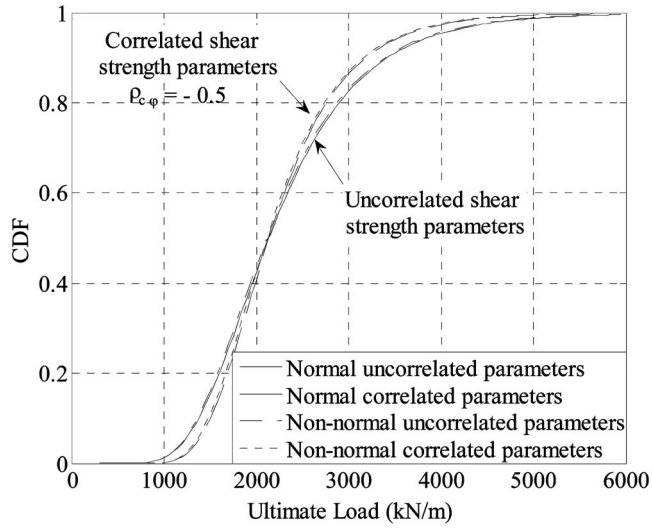

Fig. 12. Comparison of the CDFs of the ultimate load for *normal*, *nonnormal*, correlated, and uncorrelated variables

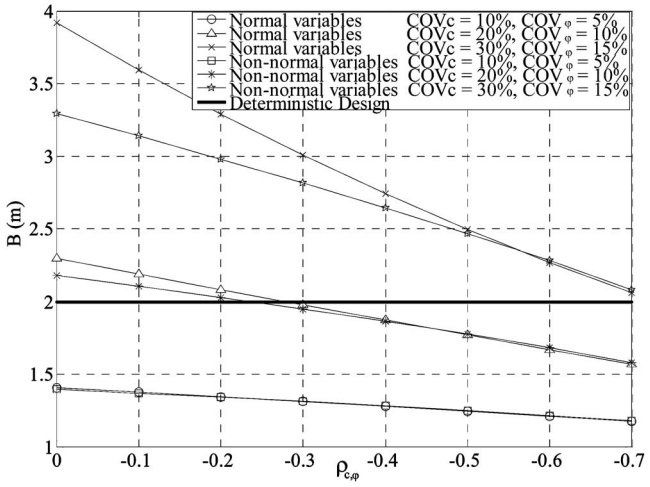

Fig. 14. Comparison between probabilistic and deterministic design

of 3. The probabilistic foundation breadth decreases with the increase of the negative correlation between the shear strength parameters and the decrease of their coefficients of variation. It can become smaller than the deterministic breadth for the common values of the soil variability (i.e., $COV_{\varphi}=10\%$, $COV_c=20\%$, $-0.7 \leq \rho_{c,\varphi} \leq -0.3$). For high values of the coefficients of variation and small correlation coefficient, the design breadth for normal variables is higher than that of nonnormal variables. This means that, for the case in hand, assuming *normal* distributions for the random variables is more conservative than assuming *nonnormal* distributions. As a conclusion, the deterministic footing breadth may be higher or lower than the reliability-based footing width, depending on the uncertainties.

Contrary to Eurocode 7, which prescribes constant values of the partial safety factors F_c and F_{φ}, the present RBD has the advantage of providing different values of these factors depending on the soil variability. These factors are the optimal ones and are determined rigorously by a maximization of the failure probability for a given soil variability. Hence, a reliability-based design has the merit of explicitly reflecting the correlation structure, the standard deviations, and the probability distributions of the underlying random variables, and of automatically seeking the design point without relying on prescribed values of partial safety factors.

Mechanism M2

The number of rigid blocks used in the $M2$ mechanism (Fig. 3) is equal to 12 since further increase in the number of blocks improves the optimal solution by less than 0.5%. For the seismic coefficient, an exponential distribution (Exp D) and an extreme value type II distribution (EVD) are used (Haldar and Mahadevan 2000). The mean value of the horizontal seismic coefficient is assumed to be 0.15. The angle of internal friction is considered to follow the beta distribution.

It was shown for the $M1$ mechanism (Fig. 13) that the failure probability of a vertically loaded footing is more sensitive to a variation of the angle of internal friction than the cohesion. For the seismically loaded footing in hand, Fig. 15 presents the effect of the randomness of the soil cohesion on the reliability index for both exponential and extreme value distributions of the seismic coefficient. In this figure, the cohesion c is assumed to be either a lognormally distributed random variable with the commonly used

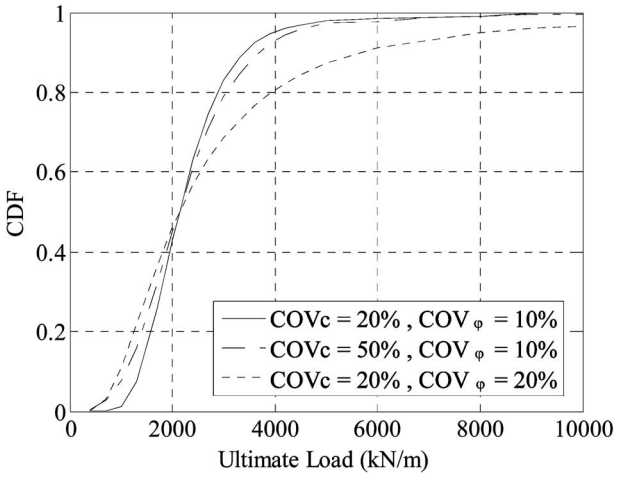

Fig. 13. Comparison of CDFs of the ultimate load for different values of the coefficients of variation

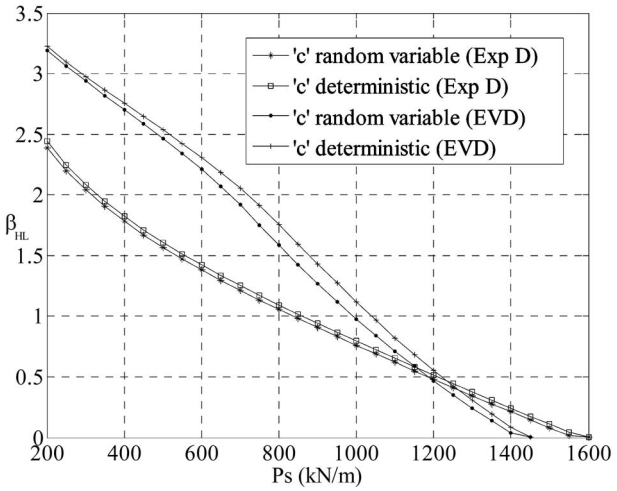

Fig. 15. Effect of the variability of c on the reliability index

Table 2. Probabilistic Results When K_h Follows the Exponential Distribution

P_S kN/m	φ^* (deg)	K_h^*	β_{HL}	$\gamma(\mu_\varphi)$	$\gamma(\mu_{K_h})$	$P_f(\%)$
200	28.58	0.70	2.44	1.02	2.03	3.87
450	28.77	0.45	1.71	1.03	2.62	6.52
700	28.84	0.32	1.25	1.06	1.95	11.45
1,000	29.01	0.22	0.80	1.09	1.34	21.41
1,300	29.40	0.15	0.37	1.20	0.47	35.33
1,600	30.01	0.10	0.00	—	—	50.00

coefficient of variation (20%) or as a deterministic parameter with value equal to the mean value (i.e., 20 kPa). One may note that whether c is random or deterministic has only a minor effect on the value of the reliability index.

Reliability Index, Failure Probability, and Sensitivity Factors

Tables 2 and 3 present the reliability results (i.e., Hasofer-Lind reliability index, the corresponding design point, the omission sensitivity factors, and the failure probability) for different values of the applied load P_S varying from small values up to the deterministic ultimate load defined earlier for both exponential and extreme value distributions on K_h. The reliability index decreases with the increase of the vertical applied load P_S. The exponential distribution on K_h gives more conservative results than the extreme value distribution on K_h. The values of the omission sensitivity factors suggest that, when the applied load is relatively small compared to the deterministic ultimate load, whether φ is random or deterministic has only a minor effect on the reliability index since $\gamma(\mu_\varphi) \approx 1$ for both types of the probability distributions on K_h. On the other hand, the randomness of the seismic coefficient has a significant effect on the reliability index. Hence, for small values of the applied load, one can neglect the uncertainty in φ. In contrast, for higher values of the applied load, the uncertainties of both the angle of internal friction and the seismic coefficient should be considered in the reliability analysis.

Probability Distribution of the Punching Safety Factor

Fig. 16 shows the CDF of the punching safety factor obtained from FORM approximation for the exponential distribution and for different values of the coefficient of variation of the extreme value distribution. It can be seen that the choice of the probability distribution on K_h significantly affects the probability distribution of the safety factor. The dispersion of F is significantly larger when an exponential distribution is assumed for the seismic coefficient.

Table 3. Probabilistic Results When K_h Follows the Extreme Value Distribution and COV_{Kh}=40%

P_S kN/m	φ^* (deg)	K_h^*	β_{HL}	$\gamma(\mu_\varphi)$	$\gamma(\mu_{K_h})$	$P_f(\%)$
200	28.86	0.71	3.22	1.02	1.54	0.06
450	28.08	0.44	2.65	1.02	1.69	0.41
700	26.90	0.27	2.05	1.10	1.18	2.00
1,000	27.08	0.16	1.11	1.45	0.97	13.25
1,300	29.15	0.14	0.31	2.18	0.54	37.96
1,450	30.00	0.13	0.00	—	—	50.00

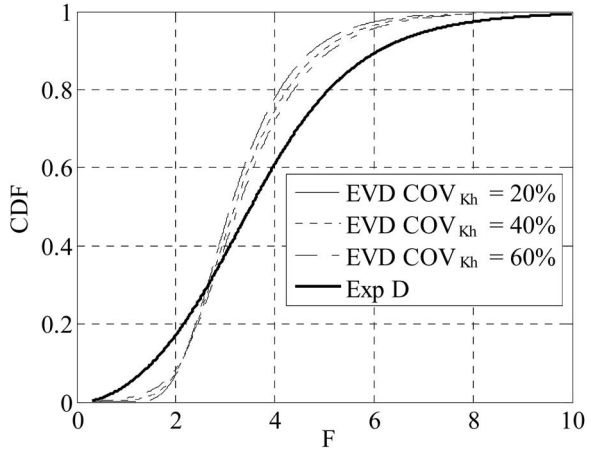

Fig. 16. CDF of the punching safety factor for P_S=450 kN/m

Probabilistic Design

For the design of a vertically loaded footing situated in seismic area, a reasonable target failure probability of 1% is used. Fig. 17 presents the probabilistic foundation breadth for the extreme value distribution on K_h and for different values of the coefficient of variation of K_h. The deterministic breadth corresponding to a safety factor of 3 is also shown. The applied load is 700 kN/m. The probabilistic foundation breadth increases with the increase of the coefficient of variation of K_h. It can be greater than the deterministic breadth for large values of the coefficient of variation.

Conclusion

A reliability-based analysis and design of a shallow strip foundation subjected to a vertical and a pseudostatic horizontal seismic loading was performed. Only the punching failure mode of the ultimate limit state was studied. Two rigorous deterministic models based on limit analysis failure mechanisms were used.

For the vertically loaded footing, the reliability index calculated based on the critical probabilistic surface is more critical than that determined using the critical deterministic surface. The reliability index decreases with the increase of the applied load P_S. The assumption of uncorrelated shear strength parameters is

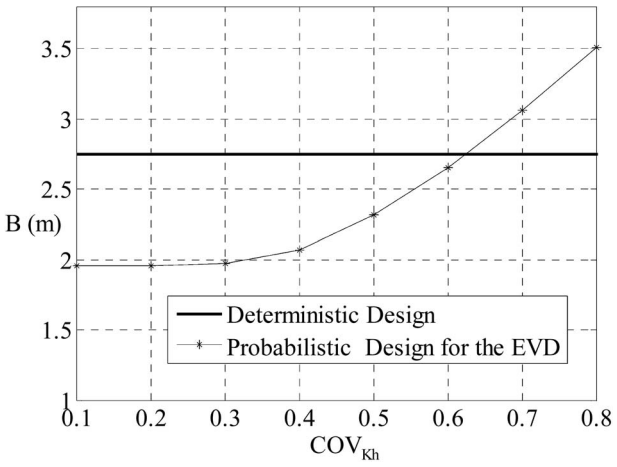

Fig. 17. Comparison between deterministic and probabilistic design

conservative in comparison to that of negatively correlated parameters. The reliability index is much more sensitive to φ than to c, especially for the case of *nonnormal* variables. The greater the scatter in φ, the higher the failure probability. This means that the accurate determination of the uncertainties of the angle of internal friction φ is important in obtaining reliable probabilistic results. FORM approximation is an acceptable approach for estimating the failure probability for the commonly used values of the soil variability. When no correlation between shear strength parameters is considered, a more spread out CDF of the ultimate load was obtained. For the case in hand, the chosen probability distribution does not significantly affect the values of the failure probability. The probabilistically-designed foundation breadth decreases with the increase of the negative correlation between the shear strength parameters and the decrease of their coefficients of variation. Contrary to Eurocode 7, which prescribes constant values of the partial safety factors F_c and F_φ, a reliability-based design has the advantage of providing different values of these factors depending on the soil variability and correlation structure. These factors are by-products of a reliability-based design and reflect parametric sensitivities from case to case in a way rigid partial safety factors cannot.

For the seismically loaded footing, the extreme value distribution was used to model the uncertainties of K_h. For values of the vertical load much below the deterministic ultimate load, one can neglect the uncertainty in φ. In contrast, for higher values of the vertical load, the uncertainties of both φ and K_h should be considered in the reliability analysis.

Acknowledgments

The first two writers would like to thank the Lebanese National Council for Scientific Research (CNRSL) and the French organization EGIDE for providing the financial support for this research.

Appendix I

The expressions of the functions f_i $(i=1,\ldots,6)$ are given as follows:

$$f_1 = \frac{\tan\theta}{2}$$

$$f_2 = \frac{\cos(\theta-\varphi)}{2\cos^2\theta\sin(\beta_1-2\varphi)} \cdot \sum_{i=1}^{n}\left[\frac{\sin\alpha_i\sin\beta_i}{\sin(\alpha_i+\beta_i)}\sin\left(\beta_i-\theta-\sum_{j=1}^{i-1}\alpha_j-\varphi\right) \cdot \prod_{j=1}^{i-1}\frac{\sin^2\beta_j\sin(\alpha_j+\beta_j-2\varphi)}{\sin^2(\alpha_j+\beta_j)\sin(\beta_{j+1}-2\varphi)}\right]$$

$$f_3 = \frac{\cos(\theta-\varphi)}{\cos\theta\sin(\beta_1-2\varphi)}\frac{\sin\beta_n}{\sin(\alpha_n+\beta_n)} \cdot \sin\left(\beta_n-\theta-\sum_{j=1}^{n-1}\alpha_j-\varphi\right) \cdot \prod_{j=1}^{n-1}\frac{\sin\beta_j\sin(\alpha_j+\beta_j-2\varphi)}{\sin(\alpha_j+\beta_j)\sin(\beta_{j+1}-2\varphi)}$$

$$f_4 = \frac{\cos(\varphi)\cos(\beta_1-\theta-\varphi)}{2\cos\theta\sin(\beta_1-2\varphi)}$$

$$f_5 = \frac{\cos(\theta-\varphi)\cos(\varphi)}{2\cos\theta\sin(\beta_1-2\varphi)} \cdot \sum_{i=1}^{n}\left[\frac{\sin\alpha_i}{\sin(\alpha_i+\beta_i)}\prod_{j=1}^{i-1}\frac{\sin\beta_j\sin(\alpha_j+\beta_j-2\varphi)}{\sin(\alpha_j+\beta_j)\sin(\beta_{j+1}-2\varphi)}\right]$$

$$f_6 = \frac{\cos(\theta-\varphi)\cos(\varphi)}{2\cos\theta\sin(\beta_1-2\varphi)} \cdot \sum_{i=2}^{n}\left[\frac{\sin(\beta_{i-1}-\beta_i+\alpha_{i-1})}{\sin(\beta_i-2\varphi)}\cdot\prod_{j=1}^{i-1}\frac{\sin\beta_j}{\sin(\alpha_j+\beta_j)} \cdot \prod_{j=1}^{i-2}\frac{\sin(\alpha_j+\beta_j-2\varphi)}{\sin(\beta_{j+1}-2\varphi)}\right]$$

Appendix II

The expressions of the functions g_i $(i=1,\ldots,6)$ are given as follows:

$$g_1 = \frac{\sin^2\beta_1}{\sin^2(\alpha_1+\beta_1)}\sum_{i=1}^{n}\left[\frac{\sin\alpha_i\sin(\alpha_i+\beta_i)}{\sin\beta_i}\sin\left(\beta_i-\varphi-\sum_{j=1}^{i-1}\alpha_j\right) \times\prod_{j=2}^{i}\frac{\sin^2\beta_j}{\sin^2(\alpha_j+\beta_j)}\prod_{j=1}^{i-1}\frac{\sin(\alpha_j+\beta_j-2\varphi)}{\sin(\beta_{j+1}-2\varphi)}\right]$$

$$g_2 = \frac{\sin^2\beta_1}{\sin^2(\alpha_1+\beta_1)}\sum_{i=1}^{n}\left[\frac{\sin\alpha_i\sin(\alpha_i+\beta_i)}{\sin\beta_i}\cos\left(\beta_i-\varphi-\sum_{j=1}^{i-1}\alpha_j\right) \times\prod_{j=2}^{i}\frac{\sin^2\beta_j}{\sin^2(\alpha_j+\beta_j)}\prod_{j=1}^{i-1}\frac{\sin(\alpha_j+\beta_j-2\varphi)}{\sin(\beta_{j+1}-2\varphi)}\right]$$

$$g_3 = \frac{\sin\beta_1}{\sin(\alpha_1+\beta_1)}\sin\left(\beta_n-\varphi-\sum_{j=1}^{n-1}\alpha_j\right) \times\prod_{j=2}^{n}\frac{\sin\beta_j}{\sin(\alpha_j+\beta_j)}\prod_{j=1}^{n-1}\frac{\sin(\alpha_j+\beta_j-2\varphi)}{\sin(\beta_{j+1}-2\varphi)}$$

$$g_4 = \frac{\sin\beta_1}{\sin(\alpha_1+\beta_1)}\cos\left(\beta_n-\varphi-\sum_{j=1}^{n-1}\alpha_j\right) \times\prod_{j=2}^{n}\frac{\sin\beta_j}{\sin(\alpha_j+\beta_j)}\prod_{j=1}^{n-1}\frac{\sin(\alpha_j+\beta_j-2\varphi)}{\sin(\beta_{j+1}-2\varphi)}$$

$$g_5 = \frac{\sin\beta_1\cos\varphi}{\sin(\alpha_1+\beta_1)}\sum_{i=1}^{n}\left[\frac{\sin\alpha_i}{\sin\beta_i}\prod_{j=2}^{i}\frac{\sin\beta_j}{\sin(\alpha_j+\beta_j)}\prod_{j=1}^{i-1}\frac{\sin(\alpha_j+\beta_j-2\varphi)}{\sin(\beta_{j+1}-2\varphi)}\right]$$

$$g_6 = \frac{\sin\beta_1\cos\varphi}{\sin(\alpha_1+\beta_1)}\sum_{i=1}^{n-1}\left[\frac{\sin(\beta_i-\beta_{i+1}+\alpha_i)}{\sin(\beta_{i+1}-2\varphi)} \times\prod_{j=2}^{i}\frac{\sin\beta_j}{\sin(\alpha_j+\beta_j)}\prod_{j=1}^{i-1}\frac{\sin(\alpha_j+\beta_j-2\varphi)}{\sin(\beta_{j+1}-2\varphi)}\right]$$

References

Calgaro, J. A. (1996). *Introduction aux Eurocodes. Sécurité des constructions et bases de la théorie de la fiabilité*, Presses de l'ENPC, Paris (in French).

Cherubini, C. (2000). "Reliability evaluation of shallow foundation bearing capacity on C′, φ′ soils." *Can. Geotech. J.*, 37, 264–269.

Christian, J., Ladd, C., and Baecher, G. (1994). "Reliability applied to slope stability analysis." *J. Geotech. Engrg.*, 120(12), 2180–2207.

Der Kiureghian, A., and Liu, P. L. (1986). "Structural reliability under incomplete probability information." *J. Eng. Mech.*, 112(1), 85–104.

Ditlevsen, O. (1981). *Uncertainty modelling: With applications to multidimensional civil engineering systems*, McGraw-Hill, New York.

El-Ramly, H., Morgenstern, N. R., and Cruden, D. M. (2002). "Probabilistic slope stability analysis for practice." *Can. Geotech. J.*, 39, 665–683.

El-Ramly, H., Morgenstern, N. R., and Cruden, D. M. (2003). "Probabilistic stability analysis of a tailing dyke on presheared clay-shale." *Can. Geotech. J.*, 40, 192–208.

Fenton, G. A., and Griffiths, D. V. (2002). "Probabilistic foundation settlement on spatially random soil." *J. Geotech. Geoenviron. Eng.*, 128(5), 381–390.

Fenton, G. A., and Griffiths, D. V. (2003). "Bearing capacity prediction of spatially random C-φ soils." *Can. Geotech. J.*, 40, 54–65.

Fenton, G. A., and Griffiths, D. V. (2005). "Three-dimensional probabilistic foundation settlement." *J. Geotech. Geoenviron. Eng.*, 131(2), 232–239.

Griffiths, D. V., and Fenton, G. A. (2001). "Bearing capacity of spatially random soil: The undrained clay Prandtl problem revisited." *Geotechnique*, 51(4), 351–359.

Griffiths, D. V., Fenton, G. A., and Manoharan, N. (2002). "Bearing capacity of rough rigid strip footing on cohesive soil: Probabilistic study." *J. Geotech. Geoenviron. Eng.*, 128(9), 743–755.

Haldar, A., and Mahadevan, S. (2000). *Probability, reliability, and statistical methods in engineering design*, Wiley, New York.

Harr, M. E. (1987). *Reliability-based design in civil engineering*, McGraw-Hill, New York.

Hasofer, A. M., and Lind, N. C. (1974). "Exact and invariant second-moment code format." *J. Engrg. Mech. Div.*, 100(1), 111–121.

Hassan, A., and Wolff, T. (1999). "Search algorithm for minimum reliability index of earth slopes." *J. Geotech. Geoenviron. Eng.*, 125(4), 301–308.

Lemaire, M. (2005). *Fiabilité des structures*, Hermes-Lavoisier, Paris (in French).

Low, B. K. (2005). "Reliability-based design applied to retaining walls." *Geotechnique*, 55(1), 63–75.

Low, B. K., Gilbert, R. B., and Wright, S. G. (1998). "Slope reliability analysis using generalized method of slices." *J. Geotech. Geoenviron. Eng.*, 124(4), 350–362.

Low, B. K., and Phoon, K. K. (2002). "Practical first-order reliability computations using spreadsheet." *Proc., Probabilistics in Geotechnics: Technical and Economic Risk Estimation*, 39–46.

Low, B. K., and Tang, W. H. (1997a). "Efficient reliability evaluation using spreadsheet." *J. Eng. Mech.*, 123(7), 749–752.

Low, B. K., and Tang, W. H. (1997b). "Probabilistic slope analysis using Janbu's generalized procedure of slices." *Comput. Geotech.*, 21(2), 121–142.

Low, B. K., and Tang, W. H. (1997c). "Reliability analysis of reinforced embankments on soft ground." *Can. Geotech. J.*, 34, 672–685.

Low, B. K., and Tang, W. H. (2004). "Reliability analysis using object-oriented constrained optimization." *Struct. Safety*, 26, 68–89.

Lumb, P. (1970). "Safety factors and the probability distribution of soil strength." *Can. Geotech. J.*, 7, 225–242.

Melchers, R. E. (1999). *Structural reliability analysis and prediction*, 2nd Ed., Wiley, New York.

Phoon, K.-K. (2004). "General non-Gaussian probability models for first-order reliability method (FORM)." *A state-of-the-art Rep.*, Int. Centre for Geohazards (ICG), Oslo, Norway.

Phoon, K.-K., and Kulhawy, F. H. (1999). "Evaluation of geotechnical property variability." *Can. Geotech. J.*, 36, 625–639.

Phoon, K.-K., Kulhawy, F. H., and Grigoriu, M. D. (2003). "Multiple resistance factor design for shallow transmission line structure foundations." *J. Geotech. Geoenviron. Eng.*, 129(9), 807–818.

Popescu, R., Deodatis, G., and Nobahar, A. (2005). "Effect of random heterogeneity of soil properties on bearing capacity." *Probab. Eng. Mech.*, 20, 324–341.

Przewlocki, J. (2005). "A stochastic approach to the problem of bearing capacity by the method of characteristics." *Comput. Geotech.*, 32, 370–376.

Rackwitz, R., and Fiessler, B. (1978). "Structural reliability under combined random load sequences." *Comput. Struct.*, 9(5), 484–494.

Soubra, A.-H. (1999). "Upper-bound solutions for bearing capacity of foundations." *J. Geotech. Geoenviron. Eng.*, 125(1), 59–68.

STRUREL. (1991). *A structural reliability analysis program: Theoretical manual*, RCP GmbH, Munchen, Germany.

Wolff, T. H. (1985). "Analysis and design of embankment dam slopes: A probabilistic approach." Ph.D. thesis, Purdue Univ., Lafayette, Ind.

Yuceman, M. S., Tang, W. H., and Ang, A. H. S. (1973). "A probabilistic study of safety and design of earth slopes." *Civil Engineering Studies, Structural Research Series, 402*, Univ. of Illinois, Urbana, Ill.